2020

Toxic effects of endoplasmic reticulum stress transducer BBF2H7-derived small peptide fragments on neuronal cells

Koji Matsuhisa

Longjie Cai

Atsushi Saito

Fumika Sakaue

Yasunao Kamikawa

See next page for additional authors

Authors

Koji Matsuhisa, Longjie Cai, Atsushi Saito, Fumika Sakaue, Yasunao Kamikawa, Sachiko Fujiwara, Rie Asada, Yukitsuka Kudo, and Kazunori Imaizumi

Brain Research 1749 (2020) 147139

Contents lists available at ScienceDirect

Brain Research

journal homepage: www.elsevier.com/locate/brainres

Research report

Toxic effects of endoplasmic reticulum stress transducer BBF2H7-derived small peptide fragments on neuronal cells

Koji Matsuhisa[a,b], Longjie Cai[a], Atsushi Saito[a,b], Fumika Sakaue[b], Yasunao Kamikawa[b], Sachiko Fujiwara[b], Rie Asada[c], Yukitsuka Kudo[d], Kazunori Imaizumi[a,*]

[a] Department of Biochemistry, Institute of Biomedical & Health Sciences, Hiroshima University, 1-2-3 Kasumi, Minami-ku, Hiroshima 734-8553, Japan
[b] Department of Stress Protein Processing, Institute of Biomedical & Health Sciences, Hiroshima University, 1-2-3 Kasumi, Minami-ku, Hiroshima 734-8553, Japan
[c] Department of Medicine, Division of Endocrinology, Metabolism, and Lipid Research, Washington University School of Medicine, St. Louis, MO 63110, USA
[d] Department of Gerontology and Geriatrics, Institute of Development, Aging and Cancer, Tohoku University, Sendai, Miyagi 980-8575, Japan

HIGHLIGHTS

- BBF2H7-derived small peptide fragments (BSP fragments) have high hydrophobicity.
- BSP fragments accelerate fibril formation of amyloid β peptide.
- Cytotoxicity of amyloid β peptide are enhanced by co-incubation with BSP fragments.
- BSP fragments could modulate pathogenicity of Alzheimer's disease.

ARTICLE INFO

Keywords:
Endoplasmic reticulum stress
BBF2H7
Alzheimer's disease

ABSTRACT

Aggregation, fibril formation, and deposition of amyloid β (Aβ) protein are believed to be the central pathogeneses of Alzheimer's disease (AD). Numerous studies have shown that fibril formation is promoted by preformed seeds at the beginning of the aggregation process. Therefore, aggregated molecules that promote fibrillization of Aβ protein as seeds could affect the pathology. We recently found that approximately 40 amino acid hydrophobic peptides, BBF2H7-derived small peptide (BSP) fragments, are generated via intramembranous cleavage under endoplasmic reticulum (ER) stress conditions. Interestingly, similar to Aβ protein, the fragments exhibit a high aggregation propensity and form fibril structures. It has been noted that ER stress is involved in the pathogenesis of AD. In this study, we examined the effect of BSP fragments on aggregation and cytotoxicity of $Aβ_{1–40}$ protein, which is generated as a major species of Aβ protein, but has a lower aggregative property than $Aβ_{1–42}$ protein. We demonstrated that BSP fragments promote aggregation of $Aβ_{1–40}$ protein. Aggregates of $Aβ_{1–40}$ protein mediated by BSP fragments also exhibited potent neurotoxicity. Our findings suggest the possibility that BSP fragments affect accumulation of Aβ proteins and are involved in the pathogenesis of AD.

1. Introduction

Alzheimer's disease (AD) is the most prevalent form of dementia. AD is characterized by misfolding, fibrillization, and accumulation of the amyloid β (Aβ) peptide, which results in the formation of extracellular senile plaques as a pathological hallmark (Masters et al., 1985). A 37–43 amino acid hydrophobic Aβ peptide is generated by sequential proteolytic processing of the amyloid precursor protein (APP) (Haass et al., 2012). APP is a type-I transmembrane protein with its N-terminus within the lumen/extracellular space and C-terminus within the cytosol. In the first step of the sequential proteolysis, β-secretase cleaves APP at the N-terminal luminal domain. This process removes a large part of the ectodomain of APP and generates a membrane-retained C-terminal fragment (CTF). CTF is processed further to Aβ and the APP intracellular domain by γ-secretase that cleaves within the transmembrane region. Aβ is located between the β- and γ-secretase cleavage sites. Heterogenous proteolysis of CTF by γ-secretase principally generates 40 and 42 amino acid peptides, $Aβ_{1–40}$ and $Aβ_{1–42}$, respectively. Although the relative abundance of $Aβ_{1–40}$ (~90%) in the brain is much greater than that of $Aβ_{1–42}$ (~10%), amyloid plaques consist predominantly of $Aβ_{1–42}$ in patients with AD (Iwatsubo et al., 1994; Roher et al., 1993). $Aβ_{1–42}$ is more hydrophobic than $Aβ_{1–40}$ and displays a

* Corresponding author.
E-mail address: imaizumi@hiroshima-u.ac.jp (K. Imaizumi).

https://doi.org/10.1016/j.brainres.2020.147139
Received 8 June 2020; Received in revised form 10 September 2020; Accepted 26 September 2020
Available online 01 October 2020

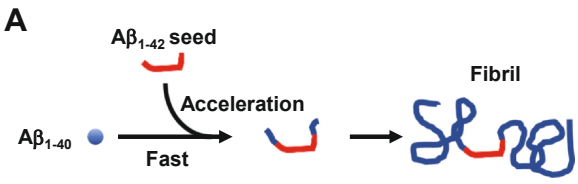

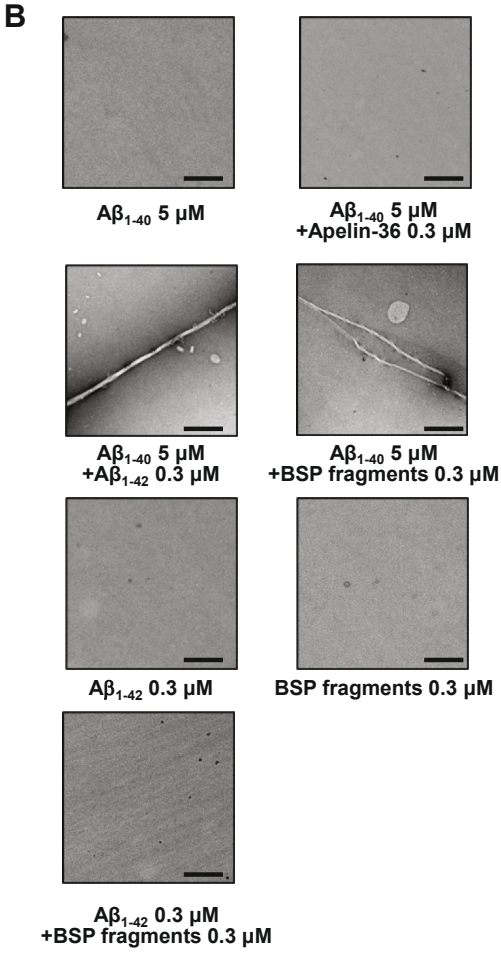

C

	Aβ1-40 + Aβ1-42	Aβ1-40 + BSP fragment
Length	959.7 ± 250.2 nm	2250.3 ± 987.1 nm *
Width	8.3 ± 1.1 nm	15.7 ± 3.8 nm **
periodicity	82.5 ± 8.8 nm	118.5 ± 19.7 nm **

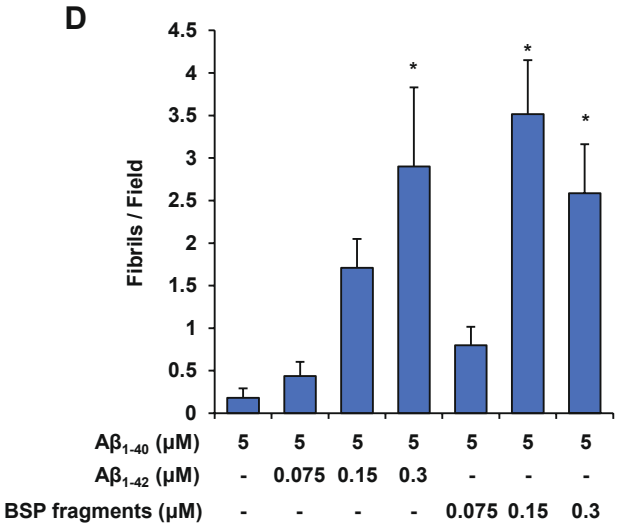

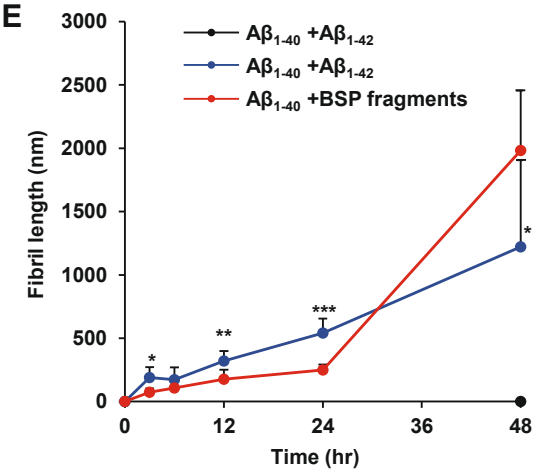

Fig. 1. BSP fragments promote fibrillization of amyloid β_{1-40}. (A) Schematic representation of the formation of amyloid fibrils accelerated by an $A\beta_{1-42}$ seed. (B) Negative-stain transmission electron microscopy micrographs of amyloid fibrils increased by addition of $A\beta_{1-42}$ or BSP fragments. Mixtures of 5 μM $A\beta_{1-40}$ and 0.15 μM $A\beta_{1-42}$, BSP fragments, or 0.3 μM Apelin-36, mixture of 0.3 μM $A\beta_{1-42}$ and 0.3 μM BSP fragments, or each peptide alone were incubated for 48 h. After incubation, the peptides were stained with uranyl acetate. Scale bar: 200 nm. (C) Length, width, and periodicity of fibrils derived from a mixture of $A\beta_{1-40}$ and $A\beta_{1-42}$, or $A\beta_{1-40}$ and BSP fragments (mean ± SD, $n = 5$). *P < 0.05, **P < 0.01 relative to a mixture of $A\beta_{1-40}$ and $A\beta_{1-42}$; significance was calculated by the Student's *t*-test. (D) Amounts of fibrils derived from a mixture of $A\beta_{1-40}$ and $A\beta_{1-42}$ or $A\beta_{1-40}$ and BSP fragments (mean ± SD, $n = 30$). *P < 0.05 relative to $A\beta_{1-40}$ alone; significance was calculated by Dunnett's method. (E) Time course of the length of fibrils derived from a mixture of $A\beta_{1-40}$ and $A\beta_{1-42}$, or $A\beta_{1-40}$ and BSP fragments (mean ± SD, $n = 5$). *P < 0.05, **P < 0.01 and ***P < 0.001 relative to a mixture of $A\beta_{1-40}$ and BSP fragments at a same time point; significance was calculated by the Student's *t*-test.

considerably higher propensity to form neurotoxic aggregates. Most familial AD-related mutations found within the transmembrane region of APP increase the $A\beta_{1-42}/A\beta_{1-40}$ ratio (Weggen and Beher, 2012). Thus, $A\beta_{1-42}$ and its aggregation are believed to be the cause of AD pathogenesis (Selkoe, 2011).

Aβ aggregation is promoted in a prion-like manner by the presence of misfolded Aβ seeds that act as a core structure of amyloid fibrils (Walker and Jucker, 2015). Local overproduction of $A\beta_{1-42}$ aggregates could induce fibrillization of abundant and normally soluble $A\beta_{1-40}$. This concept is supported by several animal models by showing accelerated Aβ pathology in host organisms after intracerebral injection of brain homogenates containing Aβ aggregates (Kane et al., 2000; Meyer-Luehmann et al., 2006). Additionally, another fibril-forming peptide, amylin, promotes fibrillization and deposition of Aβ in AD model mice (Moreno-Gonzalez et al., 2017). Hence, other aggregative molecules could affect aggregation and deposition of Aβ and modify the pathogenesis of AD.

Several studies have indicated that endoplasmic reticulum (ER) stress is closely related to AD pathology. Numerous studies have reported that various ER stress markers, such as heat shock protein 70 (also known as BiP), phosphorylated PKR-like endoplasmic reticulum kinase, phosphorylated inositol-requiring enzyme 1, and phosphorylated eukaryotic translation initiation factor 2-α, are increased in postmortem brain samples from patients with AD (Hetz and Saxena, 2017). Attenuation of ER stress by treatment with a chemical chaperone, 4-phenylbutyrate, significantly reduced the number of plaques in the hippocampus and reversed cognitive deficits in AD mouse models, which indicated a causal link between ER stress and neurodegeneration (Ricobaraza et al., 2011; Wiley et al., 2011). However, the precise mechanisms underlying ER stress and the pathogenesis of AD are not completely understood.

Recently, we found that novel small hydrophobic peptides, namely BBF2H7-derived small peptide fragments (BSP fragments), are produced in response to ER stress (Matsuhisa et al., 2020). BBF2H7, one of the OASIS family members, is a type-II transmembrane protein that is highly expressed in neurons, chondrocytes, and certain tumor tissues (Iwamoto et al., 2015; Kondo et al., 2007; Saito et al., 2009, 2014). The N-terminal segment contains a basic leucine zipper domain and projects into the cytosol. This is followed by a 20 amino acid transmembrane domain and 123 amino acid C-terminal domain that projects into the ER lumen. When unfolded proteins accumulate in the ER, BBF2H7 translocates from the ER to Golgi apparatus. In the Golgi, BBF2H7 is a substrate for two proteases, site-1 protease (S1P) and site-2 protease (S2P). S1P cleaves BBF2H7 in the luminal region. The N-terminal domain of BBF2H7 remains attached to the membrane through the transmembrane segment. The transmembrane region of this segment is then cleaved by S2P. This intramembranous cleavage releases the N-terminal fragments and 40–50 amino acid BSP fragments (Kondo et al., 2007; Matsuhisa et al., 2020). Although the cleavage enzymes are different, BSP fragments are also released by a two-step cleavage process in the luminal and transmembrane domains of the precursor, which is similar to Aβ. Additionally, BSP fragments exhibit a high aggregation propensity and form fibril-like structures (Matsuhisa et al., 2020). Thus, we hypothesized that hyper and prolonged production of BSP fragments by ER stress may affect aggregation and neurotoxicity of Aβ, which modifies AD pathogenesis.

In this study, we examined the effects of BSP fragments on fibrillization and cytotoxicity of Aβ. Furthermore, we investigated the degradation pathway of BSP fragments. Accordingly, we found that coincubation of BSP fragments promotes fibrillization and cytotoxicity of $A\beta_{1-40}$.

2. Results

2.1. BSP fragments accelerate fibril formation of $A\beta_{1-40}$

Misfolded $A\beta_{1-42}$ acts as a core structure and accelerates fibrilization of $A\beta_{1-40}$ (Fig. 1A). First, we analyzed the effect of BSP fragments on fibrillization of $A\beta_{1-40}$. An extremely high concentration of $A\beta_{1-40}$ forms fibrils. No fibrils were observed at 5 μM $A\beta_{1-40}$ in our titration experiments. To avoid fibrilization of $A\beta_{1-40}$ itself, we used 5 μM $A\beta_{1-40}$. Accordingly, 5 μM $A\beta_{1-40}$ was mixed with 0.3 μM $A\beta_{1-42}$, 0.3 μM BSP fragments, or 0.3 μM Apelin-36 and incubated at 37 ˚C for 48 h. Apelin-36 is a hydrophilic peptide and used as a negative control (Matsuhisa et al., 2020). Next, precipitates were observed by transmission electron microscopy (TEM) (Fig. 1B). TEM analysis showed that $A\beta_{1-40}$ alone did not form fibrillar structures. However, fibrils were observed after addition of $A\beta_{1-42}$, as described in a previous study (Tamaoka et al., 1994). Notably, BSP fragments accelerated fibrillization of $A\beta_{1-40}$, whereas Apelin-36 did not. We did not detect 0.3 μM $A\beta_{1-42}$ or 0.3 μM BSP fragments in aggregates. Next, we analyzed the effects of BSP fragments on fibrilization of $A\beta_{1-42}$. We examined fibrils in the incubated mixture of 0.3 μM $A\beta_{1-42}$ and 0.3 μM BSP fragments because $A\beta_{1-42}$ alone formed fibrils at the concentration higher than 0.3 μM. In contrast to $A\beta_{1-40}$ fibrilization, $A\beta_{1-42}$ fibrils were not observed after addition of BSP fragments. $A\beta_{1-42}$ fibrilization might not be affected by addition of BSP fragments because of fast aggregation of $A\beta_{1-42}$ as well as that of BSP fragments. We found that BSP fragment-promoted $A\beta_{1-40}$ fibrils were longer (approximately 2,250 nm) and wider (approximately 16 nm) than $A\beta_{1-40}$ fibrils mediated by $A\beta_{1-42}$ (length: approximately 960 nm; width: approximately 8 nm) (Fig. 1C). BSP fragments also increased the length between periodical turns in $A\beta_{1-40}$ fibrils compared with $A\beta_{1-42}$. Although the reason for these differences in acceleration of fibril formation of $A\beta_{1-40}$ by BSP fragments and $A\beta_{1-42}$ remains unclear, it is nonetheless apparent that BSP fragments have the potential to change the characteristics of $A\beta_{1-40}$ fibrils. We also examined dose-dependency of $A\beta_{1-42}$ and BSP fragments for acceleration of $A\beta_{1-40}$ fibrilization (Fig. 1D). Fibril number was increased by addition of 0.075, 0.15, and 0.3 μM $A\beta_{1-42}$ in a dose-dependent manner. Addition of BSP fragments also dose-dependently increased fibrils from 0.075 μM to 0.15 μM. Fibrils were not increased by addition of 0.3 μM BSP fragments compared with 0.15 μM BSP fragments. Next, we examined the time course of $A\beta_{1-40}$ fibril formation accelerated by $A\beta_{1-42}$ and BSP fragments (Fig. 1E). The length of $A\beta_{1-40}$ and $A\beta_{1-42}$ fibrils was linearly increased from 3 to 48 h after incubation. Fibrils of $A\beta_{1-40}$ mixed with BSP fragments were shorter than those of the mixture of $A\beta_{1-40}$ and $A\beta_{1-42}$ from 3 to 24 h. However, BSP fragment-promoted $A\beta_{1-40}$ fibrils longer than $A\beta_{1-40}$ fibrils mediated by $A\beta_{1-42}$ at 48 h. BSP fragments might strongly accelerate fibril formation of $A\beta_{1-40}$ between 24 and 48 h after incubation. Collectively, these data suggest that co-existence of BSP fragments promotes fibrillization of $A\beta_{1-40}$.

2.2. BSP fragments promote cytotoxicity of Aβ

Next, we analyzed the effect of BSP fragments on cytotoxicity of $A\beta_{1-40}$ using synthetic peptides and human neuroblastoma SK-N-SH cells. $A\beta_{1-40}$ at 5 μM was mixed with 0.15 μM $A\beta_{1-42}$, 0.15 μM BSP fragments, or 0.3 μM Apelin-36 and incubated at 37 ˚C for 24 h. The incubated peptides were then applied to SK-N-SH cells for 48 h (Fig. 2A, B). Cells treated with 5 μM $A\beta_{1-40}$ alone did not show visible morphological changes. However, 0.15 μM $A\beta_{1-42}$ slightly decreased the number of cells. $A\beta_{1-40}$ preincubated with $A\beta_{1-42}$ exhibited more potent cytotoxicity than either Aβ peptide alone, as described previously (Sowade and Jahn, 2017). Interestingly, almost all cells shrank after treatment with $A\beta_{1-40}$ coincubated with BSP fragments. A large proportion of cells were intact in the presence of 0.15 μM preincubated BSP fragments alone. Morphological changes were not observed in cells

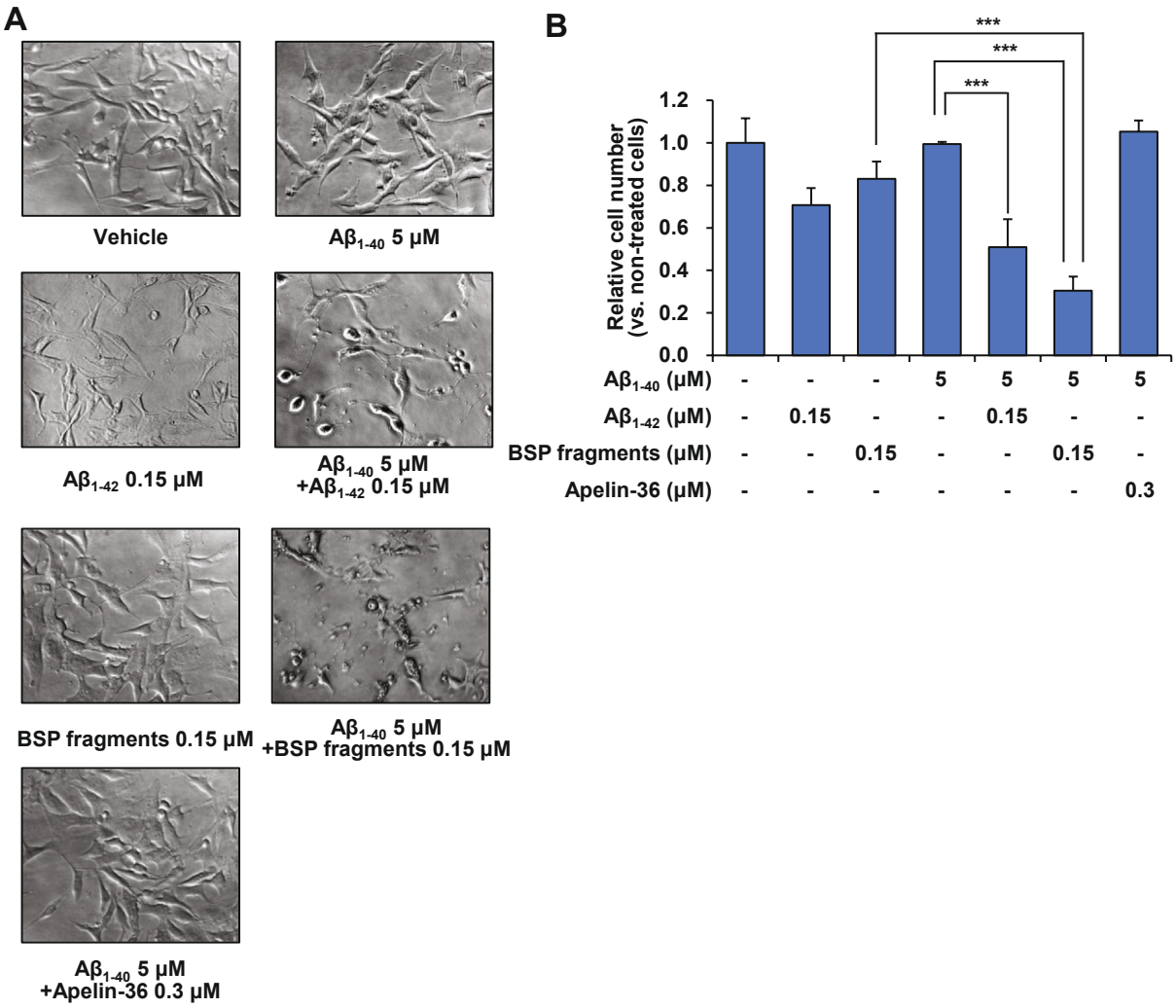

Fig. 2. BSP fragments enhance cytotoxicity of amyloid β_{1-40}. (A) Representative phase-contrast micrographs. SK-N-SH cells were cultured for 48 h in the presence of preincubated mixtures of 5 μM $A\beta_{1-40}$ and 0.15 μM $A\beta_{1-42}$, BSP fragments, or 0.3 μM Apelin-36, or each peptide alone. (B) The number of viable cells at 48 h after treatment with preincubated peptides or a mixture of peptides. Results are presented as mean relative cell counts of surviving cells compared with the untreated group ± SD ($n = 3$). ***$P < 0.001$; significance was calculated by the Tukey-Kramer method.

treated with a mixture of $A\beta_{1-40}$ and Apelin-36. Taken together, these results indicate that BSP fragments enhance the cytotoxicity of $A\beta_{1-40}$.

2.3. BSP fragments also exhibit cytotoxicity

BSP fragments have similar characteristics to those of Aβ. Accordingly, BSP fragments may directly cause cytotoxicity. To investigate the potential contribution of BSP fragments to neurodegeneration, we examined their cytotoxicity. BSP fragments were preincubated at 37 °C for 24 h and then applied to SK-N-SH cells for 48 h. A large proportion of cells were intact, but slightly decreased in number in the presence of 5 μM preincubated BSP fragments (Fig. 3A, B). The cells shrank after addition of 10 or 20 μM fragments. Moreover, treatment with the above 10 μM preincubated peptides significantly decreased cell survival. These results indicate that aggregated BSP fragments themselves are cytotoxic molecules.

2.4. BSP fragments are degraded through the lysosomal degradation pathway

Next, we analyzed the expression levels of full length and N-terminal fragments of BBF2H7, BSP fragments, and ER stress markers in SK-N-SH cells transfected with BBF2H7 under ER stress conditions induced by ER stressor thapsigargin (Tg) by Western blotting. In mammalian cells, three major ER stress transducers have been well established: PKR-like endoplasmic reticulum kinase, inositol-requiring enzyme 1, and ATF6 (Harding et al., 1999; Tirasophon et al., 1998; Yoshida et al., 2000). These transducers induce expression of C/EBP homologous protein (CHOP), spliced form of X-box binding protein 1 (XBP1s), and BiP/Grp78, respectively (Ron and Walter, 2007). Therefore, we analyzed the expression levels of these proteins as ER stress markers. BiP was increased from 12 to 24 h after treatment with Tg (Fig. 4A). Treatment with Tg induced expression of CHOP and XBP1s at 6 h, which decreased gradually from 12 to 24 h. The 80 kDa full length BBF2H7 and 60 kDa N-terminal fragments were elevated gradually from 6 h after treatment, which indicated cleavage of BBF2H7. BSP fragments were also increased after treatment with Tg for 12 h, which followed the increase in N-termini. These data indicate that BSP fragments are produced after induction of CHOP and XBP1s, and that production of BSP fragments might be sustained under ER stress conditions. Furthermore, we investigated the degradation pathway of BSP fragments. SK-N-SH cells transfected with BBF2H7 were treated with Tg with or without proteasome inhibitor MG132 or lysosomal inhibitor bafilomycin A1 (BafA1). Next, we performed Western blotting using anti-BBF2H7 N-terminus and -BSP fragment antibodies. Full length and N-terminal fragments of BBF2H7 were increased gradually in Tg-

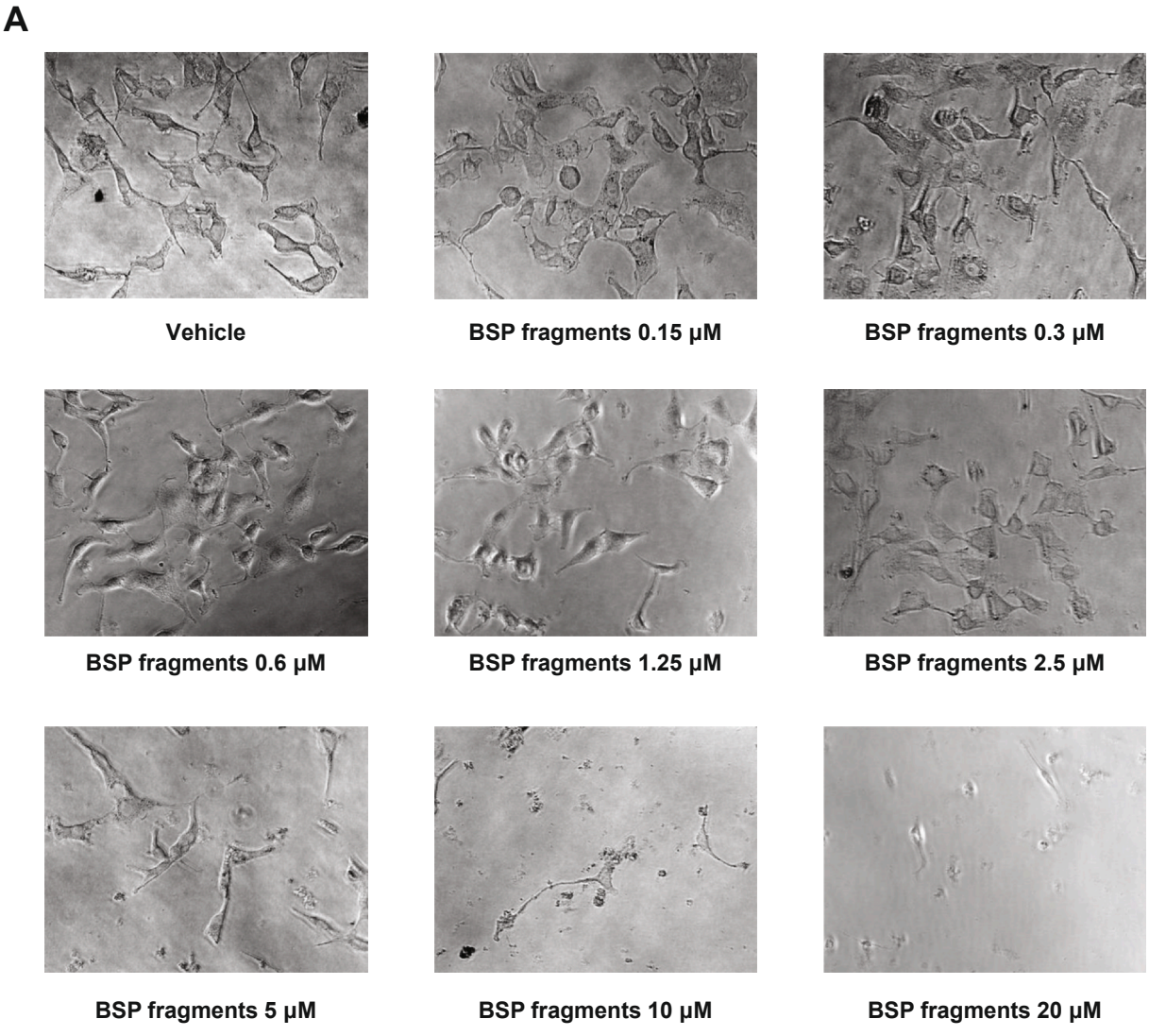

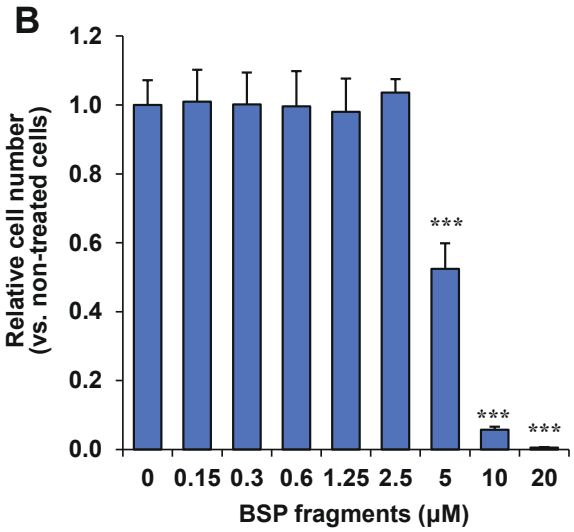

Fig. 3. BSP fragments exhibit cytotoxicity. (A) Representative phase-contrast micrographs. SK-N-SH cells were cultured for 48 h in the presence of 0.15, 0.3, 0.6, 1.25, 2.5, 5, 10, and 20 μM preincubated BSP fragments. (B) The number of viable cells at 48 h after treatment with preincubated BSP fragments. Results are presented as mean relative cell counts of surviving cells compared with the untreated group ± SD ($n = 3$). ***$P < 0.001$ relative to control; significance was calculated by Dunnett's method.

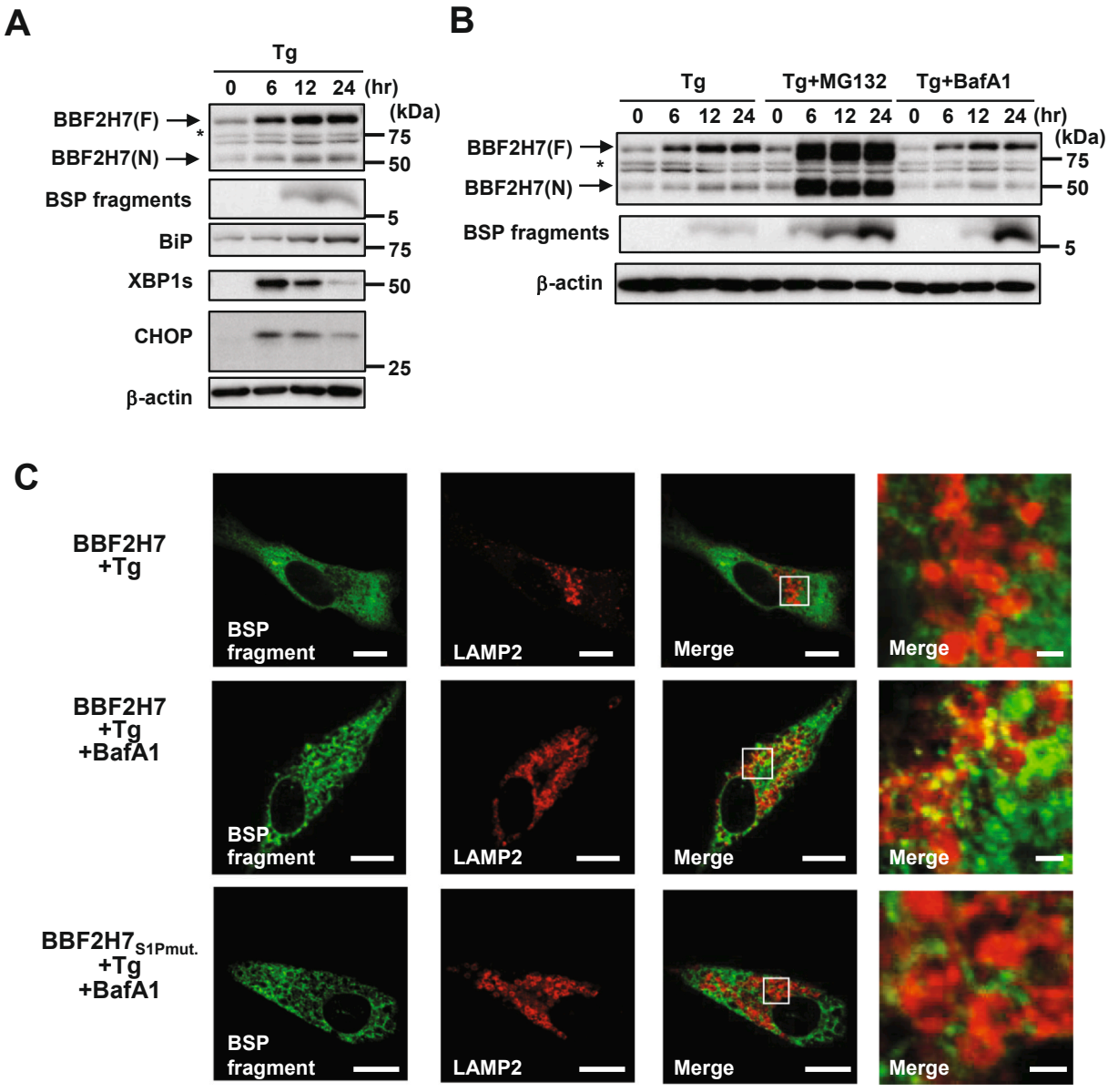

Fig. 4. BSP fragments are degraded via the lysosomal pathway. (A) Western blotting of BBF2H7 N-terminal fragments, BSP fragments and ER stress markers BiP, spliced form of XBP1 (XBP1s) and CHOP in SK-N-SH cells expressing BBF2H7. Cells were treated with 1 μM thapsigargin (Tg) for the indicated times. Lysates were subjected to Western blotting using anti-BBF2H7 N-terminus, anti-KDEL (to detect BiP), anti-XBP1s, and anti-CHOP antibodies. To detect BSP fragments, lysates were immunoprecipitated using an anti-BSP fragment antibody followed by Western blotting with the same antibody. (B) Western blotting of BBF2H7 N-terminal and BSP fragments in SK-N-SH cells expressing BBF2H7. Cells were treated with 1 μM Tg alone or together with 10 μM MG132 or 100 nM bafilomycin A1 (BafA1) for the indicated times. (C) Immunofluorescence staining of BSP fragment (Green) and lysosome-associated membrane protein-2 (LAMP2; Red) in SK-N-SH cells expressing BBF2H7 or BBF2H7$_{S1Pmut.}$. Cells were treated with 1 μM Tg alone or together with 100 nM BafA1 for 12 h. Right most panels show higher magnification images in the boxes shown in merged panel. Scale bars: 10 μm (BSP fragment, LAMP2, and lower magnification merged panels) and 1 μm (higher magnification images).

treated cells (Fig. 4B). BSP fragments appeared at 12 h after treatment. Treatment of cells with Tg and MG132 resulted in a dramatic increase in BSP fragments. Levels of full length BBF2H7 and N-terminal fragments were also elevated in these cells. BBF2H7 is degraded by the ubiquitin–proteasome system under normal conditions (Kondo et al., 2012). Stabilization of full length BBF2H7 by inhibition of the proteasome leads to an increase in the N-terminal and BSP fragments. Co-treatment with BafA1 did not increase the levels of N-terminal fragments compared with Tg-treated cells, which indicated that cleavage of BBF2H7 was not affected. However, levels of BSP fragments were increased significantly by lysosomal inhibition. These data indicate that BSP fragments were degraded in lysosomes. Additionally, we performed immunofluorescence staining of SK-N-SH cells transfected with BBF2H7 (Fig. 4B). Immunoreactivities of BSP fragments did not overlap with those of lysosome-associated membrane protein 2 (LAMP2; a lysosomal marker) in cells treated with Tg. BSP fragments accumulated in LAMP2-positive lysosomes after inhibition of lysosomal functions by cotreatment with BafA1. The anti-BSP fragment antibody used in this study also detects full length BBF2H7. BSP fragments were not produced from BBF2H7 mutated in its S1P recognition site (BBF2H7$_{S1Pmut.}$; RNLL to ANLV) (Matsuhisa et al., 2020). Then, we analyzed the immunoreactivities of BSP fragments in SK-N-SH cells transfected with BBF2H7$_{S1Pmut.}$. The signals of BSP fragments did not overlap with those of LAMP2 in cells expressing BBF2H7$_{S1Pmut.}$ in spite of treating the cells with Tg and BafA1. Therefore, these findings suggest that BSP fragments are constitutively degraded in lysosomes.

3. Discussion

We have shown that BSP fragments promote fibrillization of $A\beta_{1-40}$ (Fig. 1B). Formation of amyloid fibrils is described by the seeding-nucleation polymerization model (Jarrett and Lansbury, 1993). First, monomeric Aβ is incorrectly folded and forms small oligomeric aggregates. The aggregates act as "seeds" in fibrilization of Aβ. This aggregation process is thermodynamically unfavorable. Then, the seeds rapidly recruit and misfold the other Aβ monomers. The misfolded Aβ monomers bind to the seeds and form fibrils. Formation of seeds is a rate-limiting step in fibrillization. Several studies have shown that the aggregates derived from different proteins such as prion protein, tau, and α-synuclein act as preformed seeds, which accelerate fibril formation of Aβ (Morales et al., 2013). It has been proposed that the amyloid structure promotes misfolding of other amyloidogenic proteins (Makarava and Baskakov, 2012). Our previous study revealed that BSP fragments easily aggregate and form fibril structures similar to Aβ and other amyloidogenic proteins (Matsuhisa et al., 2020). Aggregated BSP fragments could recruit monomeric Aβ and change its conformation to a misfolded structure as preformed seeds, which accelerates fibril formation.

Amyloid fibrils are commonly twisted and exhibit periodical turns. TEM analysis revealed the twisted structures of $A\beta_{1-40}$ fibrils formed by coincubation with BSP fragments (BSP-$A\beta_{1-40}$ fibrils) (Fig. 1C). The length between turns was longer than that of fibrils mediated by $A\beta_{1-42}$ ($A\beta_{1-42}$-$A\beta_{1-40}$ fibrils). Previous studies have shown that morphological differences of Aβ fibrils correlate with their neurotoxicity (Meyer-Luehmann et al., 2006; Petkova et al., 2005; Stöhr et al., 2012). Aβ fibrils with a short distance between turns exhibit low cytotoxicity compared with those with a long distance between turns (Kumar et al., 2015). The length between turns of BSP-$A\beta_{1-40}$ fibrils was longer than those of $A\beta_{1-42}$-$A\beta_{1-40}$ fibrils and $A\beta_{1-42}$ fibrils (Matsuhisa et al., 2020). Cell survival assays showed that BSP-$A\beta_{1-40}$ fibrils exhibited more potent cytotoxicity than $A\beta_{1-42}$-$A\beta_{1-40}$ fibrils (Fig. 2B). Taken together, these findings suggest that BSP fragments affect the cytotoxicity of Aβ fibrils by modulating their periodical turns.

BSP fragments themselves also decreased neuronal cell viability (Fig. 3A, B). Although the cytotoxic mechanisms of Aβ are still not fully determined, some researchers have proposed that Aβ cause membrane damage through the formation of stable pores on the membrane, which result in severe neurotoxicity (Kotler et al., 2014). Other amyloidogenic proteins including 37 amino acid peptide amylin also exhibit cytotoxicity through the same mechanism (Cheng et al., 2013). Hydrophobic interactions between amyloidogenic proteins including Aβ and membranes is essential for their cytotoxicity. A previous study has suggested that the fibril-forming propensity is partly related to the assembly of Aβ within the membrane (Yip and McLaurin, 2001). BSP fragments also contain a highly hydrophobic N-terminal region and form a fibril structure similar to Aβ (Matsuhisa et al., 2020). Therefore, it is possible that BSP fragments disrupt cell membrane integrity and cause cell death via an interaction between their N-terminal hydrophobic region and membranes. Additionally, Aβ has been reported to exhibit cytotoxicity through production of reactive oxygen species (ROS) (Uttara et al., 2009). Aβ binds to metal ions, such as Cu, Zn, and Fe, via the imidazole ring of His residues (Cheignon et al., 2018). The Aβ-metal complex plays an important role in production of ROS. Another amyloidogenic peptide, amylin, also binds to Cu ions via the His residue and the complex produces ROS (Seal and Dey, 2018). BSP fragments contain a His residue in the luminal region. Taken together, another possible cytotoxic mechanism of BSP fragments is that the fragments form a complex with metal ions via the His residue and produce ROS, which results in cell death.

BSP fragments accumulate and are metabolically degraded in the lysosome (Fig. 4). Many previous investigations have found lysosomal dysfunction in patients with AD (Whyte et al., 2017). It is natural that BSP fragments accumulate in the lysosome because of impaired lysosomal degradation in the brain of AD patients. It is known that Aβ resides at the outer membrane of multivesicular bodies (MVBs) in the neurons of AD patients (Takahashi et al., 2002). However, it has been frequently observed that Aβ accumulates in the lysosome of patients with AD (Zheng et al., 2012). MVBs fuse with the lysosome and then their contents undergo degradation. Thus, dysfunction of the lysosome reduces degradation of Aβ, which results in accumulation in the lysosome. Lysosomal accumulation of BSP fragments suggests the possibility that the fragments act as seeds for Aβ fibrils and promote fibril formation in the lysosome. Therefore, it would be interesting to analyze the promoting effects of BSP fragments on aggregation of Aβ *in vivo*.

Interestingly, ER stress markers appeared even in morphologically healthy neurons of patients in the early stages of AD (Hoozemans et al., 2009). It has also been reported that the number of neurons containing phosphorylated PKR-like endoplasmic reticulum kinase, which is an ER stress sensor, correlates with the pathological stage in post-mortem AD brains (Hoozemans et al., 2009). These observations indicate that ER stress is induced in the early stages of AD and the ER stress response is activated as the disease progresses. Because production of BSP fragments is dependent on ER stress, the fragments could be sustainably produced in neurons from the early stages of AD. Taken together, it is conceivable that long term ER stress and lysosomal dysfunction could synergistically cause overproduction and accumulation of BSP fragments, which accelerates fibril formation of Aβ.

In conclusion, our results suggest the possibility that BSP fragments promote deposition of Aβ as a core structure of amyloid fibrils. We believe that our findings may contribute to a better understanding of the pathological mechanisms and the development of novel therapeutic approaches of AD. *In vivo* analyses of the significance of BSP fragments in AD pathogenesis may provide novel insights into the aggregation mechanisms of Aβ.

4. Experimental procedure

4.1. Cell culture, reagents, and plasmids

SK-N-SH cells were maintained in α-modified Eagle's medium (Gibco, Thermo Fisher Scientific, Waltham, MA, USA) supplemented with 10% FBS at 37 °C in a humidified atmosphere with 5% CO_2. For cell treatments, 1 μM thapsigargin (Tg) (Wako, Osaka, Japan), 10 μM MG132 (Wako), and 100 nM bafilomycinA1 (Sigma–Aldrich, St Louis, MO, USA) were used. The major species of BSP fragment (CFAVAFG-SFFQGYGPYPSATKMALPSQHPLSEPYTASVVRSRNLL) was synthesized by Peptide Institute (Osaka, Japan). $A\beta_{1-40}$ and $A\beta_{1-42}$ peptides were purchased from Peptide Institute (Osaka, Japan). Apelin-36 was purchased from Cayman Chemical Company (Ann Arbor, MI, USA).

The pcDNA3.1(+) vector expressing BBF2H7 was constructed previously (Kondo et al., 2007). Transfection of the expression vector was performed using ScreenFectA (Wako) in accordance with the manufacturer's protocol. Cells transfected with the expression vector were used in experiments at 24 h after transfection.

4.2. Protein preparation and Western blotting

Proteins were extracted from cells in cell lysis buffer containing 10 mM Tris-HCl (pH 7.4), 5 mM ethylenediaminetetraacetic acid (EDTA), 150 mM NaCl, 1% Triton X-100, and protease inhibitor cocktail Set V (Wako) at 4 °C. Lysates were incubated on ice for 15 min. After centrifugation at 15,000 × *g* for 15 min, the protein concentrations of supernatants were determined using a bicinchoninic acid assay kit (Thermo Fisher Scientific). Equal amounts of proteins (10 μg) were subjected to sodium dodecyl sulfate–polyacrylamide gel electrophoresis (SDS-PAGE). For immunoblotting, the following antibodies were used: anti-β-actin (1:10000, S5441, Sigma-Aldrich), rabbit polyclonal anti-BBF2H7-N antibody (1:2000), and rabbit polyclonal anti-BSP fragment (1:1000) [generated as described previously; (Matsuhisa et al., 2020;

Saito et al., 2009)]. Samples were subjected to SDS–PAGE followed by Western blotting.

4.3. Immunofluorescence staining

SK-N-SH cells were grown on coverslips and fixed in 4% paraformaldehyde for 30 min. After fixation, the cells were permeabilized in 0.1% Triton-X 100 for 5 min, followed by treatment with 10% goat serum for 60 min. These procedures were performed at room temperature (25 ˚C). The following antibodies were used: anti-BSP fragment (1:200) and anti-lysosome-associated membrane protein 2 (LAMP2) (1:200, 555803, BD Biosciences, Franklin Lakes, NJ, USA). Cells were visualized under an FV1000D confocal microscope (Olympus, Tokyo, Japan).

4.4. Immunoprecipitation

Cells were lysed in cell lysis buffer (10 mM Tris-HCl, pH7.4, 5 mM EDTA, 150 mM NaCl, 1% Triton X-100, and Protease inhibitor cocktail set V) for 15 min. Cell lysates were incubated with the anti-BSP fragment antibody (10 μg/1 × 10^6 cells) and Protein G Agarose Beads (Merck Millipore, Burlington, MA, USA) at 4 ˚C overnight. The beads were then rinsed three times with wash buffer (10 mM Tris-HCl, pH 7.4, 5 mM EDTA, 150 mM NaCl, and 0.1% Triton X-100). Immunoprecipitates were boiled in Laemmli SDS-PAGE sample buffer, followed by Western blotting using the anti-BSP fragment (1:1000) antibody.

4.5. Transmission electron microscopy (TEM) for observation of fibril formation of peptides

Fibril formation and acceleration of $A\beta_{1-40}$ fibrillization of BSP fragments were analyzed using a modification of previously published protocols (Yanagida et al., 2009). Briefly, synthetic BSP fragments were dissolved in dimethyl formamide to a concentration of 10 mM. The resultant peptides were mixed in 50 mM potassium phosphate buffer (pH 7.4). Diluted peptides were then incubated at 37 ˚C for 0, 3, 6, 12, 24, or 48 h. After incubation, the peptides were centrifuged for 10 min at 20,600 × *g*, and precipitated fibrils were analyzed by TEM.

Precipitated fibrils were suspended in 10 μl distilled water. Samples (3 μl) were applied to carbon-coated Slidefilm SLC-C15 (STEM, Tokyo, Japan) and incubated for 3 min at room temperature. Excess samples were absorbed with filter paper, after which an equal volume of uranyl acetate solution was added. After incubation for 2 min at room temperature, the solution was removed and the grid was dried in air. Samples were examined under a JEM-1400 transmission electron microscope (JEOL, Tokyo, Japan).

4.6. Cell survival assay

BSP fragments, Aβ peptides, or a mixture of Aβ, BSP fragments, or Apelin-36 were preincubated at 37 ˚C for 24 h in 50 mM potassium phosphate buffer (pH 7.4). SK-N-SH cells were treated with preincubated peptides for 48 h. The number of surviving cells was counted on the basis of morphological changes.

4.7. Statistical analysis

Statistical comparisons were made using the Student's *t*-test, Tukey–Kramer method, or Dunnett's method. The statistical significance of differences was determined by $P < 0.05$.

CRediT authorship contribution statement

Koji Matsuhisa: Investigation, Funding acquisition, Writing - original draft, Writing - review & editing. **Longjie Cai:** Investigation, Validation. **Atsushi Saito:** Validation, Funding acquisition, Writing - review & editing. **Fumika Sakaue:** Writing - original draft. **Yasunao Kamikawa:** Writing - original draft. **Sachiko Fujiwara:** Writing - original draft. **Rie Asada:** Writing - original draft. **Yukitsuka Kudo:** Writing - original draft. **Kazunori Imaizumi:** Conceptualization, Funding acquisition, Supervision, Project administration, Writing - review & editing.

Acknowledgements

This study was supported by grants from the Japan Society for the Promotion of Science KAKENHI (JP16K18395, JP17H01424, JP17H06416, and JP19K16076), Japan Intractable Diseases Research Foundation, The Uehara Memorial Foundation, Mitsui Sumitomo Insurance Welfare Foundation, Terumo Foundation for Life Sciences and Arts, and the Sumitomo Electric Industries Group Corporate Social Responsibility Foundation. Transmission electron microscopy was performed by Dr. Kanae Koike at the Electron Microscopy Service, Center for Gene Science, Hiroshima University (Hiroshima, Japan). We thank Mitchell Arico from Edanz Group (https://en-author-services.edanzgroup.com/ac) for editing a draft of this manuscript.

Author contributions

K.M., L.C., and A.S. performed experiments. K.I. supervised the project. K.M., A.S., and K.I. designed the experiments, analyzed data, and wrote the manuscript. F.S., Yasunao Kamikawa, S.F., R.A., and Yukitsuka Kudo provided substantial input into the writing of the manuscript.

References

Cheignon, C., Tomas, M., Bonnefont-Rousselot, D., Faller, P., Hureau, C., Collin, F., 2018. Oxidative stress and the amyloid beta peptide in Alzheimer's disease. Redox Biol. 14, 450–464.
Cheng, B., Gong, H., Xiao, H., Petersen, R.B., Zheng, L., Huang, K., 2013. Inhibiting toxic aggregation of amyloidogenic proteins: A therapeutic strategy for protein misfolding diseases. BBA 1830, 4860–4871.
Haass, C., Kaether, C., Thinakaran, G., Sisodia, S., 2012. Trafficking and proteolytic processing of APP. Cold Spring Harb Perspect Med. 2, a006270.
Harding, H.P., Zhang, Y., Ron, D., 1999. Protein translation and folding are coupled by an endoplasmic-reticulum-resident kinase. Nature 397, 271–274.
Hetz, C., Saxena, S., 2017. ER stress and the unfolded protein response in neurodegeneration. Nat Rev Neurol. 13, 477–491.
Hoozemans, J.J., van Haastert, E.S., Nijholt, D.A., Rozemuller, A.J., Eikelenboom, P., Scheper, W., 2009. The unfolded protein response is activated in pretangle neurons in alzheimer's disease hippocampus. Am. J. Pathol. 174, 1241–1251.
Iwamoto, H., Matsuhisa, K., Saito, A., Kanemoto, S., Asada, R., Hino, K., Takai, T., Cui, M., Cui, X., Kaneko, M., Arihiro, K., Sugiyama, K., Kurisu, K., Matsubara, A., Imaizumi, K., 2015. Promotion of cancer cell proliferation by cleaved and secreted luminal domains of ER stress transducer BBF2H7. PLoS ONE 10, e0125982.
Iwatsubo, T., Odaka, A., Suzuki, N., Mizusawa, H., Nukina, N., Ihara, Y., 1994. Visualization of a beta 42(43) and a beta 40 in senile plaques with end-specific a Beta monoclonals: evidence that an initially deposited species is a beta. Neuron 42 (43), 13.
Jarrett, J.T., Lansbury, P.T., 1993. Seeding "One-Dimensional Crystallization" of amyloid: a pathogenic mechanism in alzheimer's disease and scrapie? Cell 73, 1055–1058.
Kane, M.D., Lipinski, W.J., Callahan, M.J., Bian, F., Durham, R.A., Schwarz, R.D., Roher, A.E., Walker, L.C., 2000. Evidence for seeding of beta -amyloid by intracerebral infusion of Alzheimer brain extracts in beta -amyloid precursor protein-transgenic mice. J. Neurosci. 20.
Kondo, S., Saito, A., Hino, S., Murakami, T., Ogata, M., Kanemoto, S., Nara, S., Yamashita, A., Yoshinaga, K., Hara, H., Imaizumi, K., 2007. BBF2H7, a novel transmembrane bZIP transcription factor, is a new type of endoplasmic reticulum stress transducer. Mol. Cell. Biol. 27, 1716–1729.
Kondo, S., Hino, S.I., Saito, A., Kanemoto, S., Kawasaki, N., Asada, R., Izumi, S., Iwamoto, H., Oki, M., Miyagi, H., Kaneko, M., Nomura, Y., Urano, F., Imaizumi, K., 2012. Activation of OASIS family, ER stress transducers, is dependent on its stabilization. Cell Death Differ. 19, 1939–1949.
Kotler, S.A., Walsh, P., Brender, J.R., Ramamoorthy, A., 2014. Differences between amyloid-β aggregation in solution and on the membrane: insights into elucidation of the mechanistic details of Alzheimer's disease. Chem. Soc. Rev. 43, 6692–6700.
Kumar, J., Namsechi, R., Sim, V.L., 2015. Structure-based peptide design to modulate amyloid beta aggregation and reduce cytotoxicity. PLoS ONE 10, e0129087.
Makarava, N., Baskakov, I.V., 2012. Genesis of tramsmissible protein states via deformed templating. Prion. 6, 252–255.

Masters, C.L., Simms, G., Weinman, N.A., Multhaup, G., McDonald, B.L., Beyreuther, K., 1985. Amyloid plaque core protein in Alzheimer disease and Down syndrome. Proc. Natl. Acad. Sci. USA 82, 4245–4249.
Matsuhisa, K., Saito, A., Cai, L., Kaneko, M., Okamoto, T., Sakaue, F., Asada, R., Urano, F., Yanagida, K., Okochi, M., Kudo, Y., Matsumoto, M., Nakayama, K.I., Imaizumi, K., 2020. Production of BBF2H7-derived small peptide fragments via endoplasmic reticulum stress-dependent regulated intramembrane proteolysis. FASEB J. 34, 865–880.
Meyer-Luehmann, M., Coomaraswamy, J., Bolmont, T., Kaeser, S., Schaefer, C., Kilger, E., Neuenschwander, A., Abramowski, D., Frey, P., Jaton, A.L., Vigouret, J.M., Paganetti, P., Walsh, D.M., Mathews, P.M., Ghiso, J., Staufenbiel, M., Walker, L.C., Jucker, M., 2006. Exogenous induction of cerebral beta-amyloidogenesis is governed by agent and host. Science 313, 1781–1784.
Morales, R., Moreno-Gonzalez, I., Soto, C., 2013. Cross-seeding of misfolded proteins: implications for etiology and pathogenesis of protein misfolding diseases. PLoS Pathog. 9, e1003537.
Moreno-Gonzalez, I., Edwards Iii, G., Salvadores, N., Shahnawaz, M., Diaz-Espinoza, R., Soto, C., 2017. Molecular interaction between type 2 diabetes and Alzheimer's disease through cross-seeding of protein misfolding. Mol. Psychiatry 22, 1327–1334.
Petkova, A.T., Leapman, R.D., Guo, Z., Yau, W.M., Mattson, M.P., Tycko, R., 2005. Self-propagating, molecular-level polymorphism in alzheimer's beta-amyloid fibrils. Science 307, 262–265.
Ricobaraza, A., Cuadrado-Tejedor, M., Garcia-Osta, A., 2011. Long-term phenylbutyrate administration prevents memory deficits in Tg2576 mice by decreasing abeta. Front Biosci (Elite Ed). 3, 1375–1384.
Roher, A.E., Lowenson, J.D., Clarke, S., Woods, A.S., Cotter, R.J., Gowing, E., Ball, M.J., 1993. beta-Amyloid-(1–42) is a major component of cerebrovascular amyloid deposits: implications for the pathology of Alzheimer disease. Proc. Natl. Acad. Sci. USA 90, 10836–10840.
Ron, D., Walter, P., 2007. Signal integration in the endoplasmic reticulum unfolded protein response. Nat. Rev. Mol. Cell Biol. 8, 519–529.
Saito, A., Hino, S., Murakami, T., Kanemoto, S., Kondo, S., Saitoh, M., Nishimura, R., Yoneda, T., Furuichi, T., Ikegawa, S., Ikawa, M., Okabe, M., Imaizumi, K., 2009. Regulation of endoplasmic reticulum stress response by a BBF2H7-mediated Sec23a pathway is essential for chondrogenesis. Nat. Cell Biol. 11, 1197–1204.
Saito, A., Kanemoto, S., Zhang, Y., Asada, R., Hino, K., Imaizumi, K., 2014. Chondrocyte proliferation regulated by secreted luminal domain of ER stress transducer BBF2H7/CREB3L2. Mol. Cell 53, 127–139.
Seal, M., Dey, S.G., 2018. Active-Site Environment of Copper-Bound Human Amylin Relevant to Type 2 Diabetes. Inorg. Chem. 57, 129–138.
Selkoe, D.J., 2011. Alzheimer's disease. Cold Spring Harbor Perspecti. Biol. 3.
Sowade, R.F., Jahn, T.R., 2017. Seed-induced acceleration of amyloid-β mediated neurotoxicity in vivo. Nat. Commun. 8.
Stöhr, J., Watts, J.C., Mensinger, Z.L., Oehler, A., Grillo, S.K., DeArmond, S.J., Prusiner, S.B., Giles, K., 2012. Purified and synthetic alzheimer's amyloid beta (aβ) prions. Proc Natl Acad Sci U S A. 109, 11025–11030.
Takahashi, R.H., Milner, T.A., Li, F., Nam, E.E., Edgar, M.A., Yamaguchi, H., Beal, M.F., Xu, H., Greengard, P., Gouras, G.K., 2002. Intraneuronal alzheimer abeta42 accumulates in multivesicular bodies and is associated with synaptic pathology. Am. J. Pathol. 161, 1869–1879.
Tamaoka, A., Kondo, T., Odaka, A., Sahara, N., Sawamura, N., Ozawa, K., Suzuki, N., Shoji, S., Mori, H., 1994. Biochemical evidence for the long-tail form (A beta 1–42/43) of amyloid beta protein as a seed molecule in cerebral deposits of Alzheimer's disease. Biochem. Biophys. Res. Commun. 205, 834–842.
Tirasophon, W., Welihinda, A.A., Kaufman, R.J., 1998. A stress response pathway from the endoplasmic reticulum to the nucleus requires a novel bifunctional protein kinase/endoribonuclease (Ire1p) in mammalian cells. Genes Dev. 12, 1812–1824.
Uttara, B., Singh, A.V., Zamboni, P., Mahajan, R.T., 2009. Oxidative Stress and Neurodegenerative Diseases: A Review of Upstream and Downstream Antioxidant Therapeutic Options. Curr. Neuropharmacol. 7, 65–74.
Walker, L.C., Jucker, M., 2015. Neurodegenerative diseases: expanding the prion concept. Annu. Rev. Neurosci. 38, 87–103.
Weggen, S., Beher, D., 2012. Molecular consequences of amyloid precursor protein and presenilin mutations causing autosomal-dominant Alzheimer's disease. Alzheimers Res Ther. 4, 9.
Whyte, L.S., Lau, A.A., Hemsley, K.M., Hopwood, J.J., Sargeant, T.J., 2017. Endo-lysosomal and autophagic dysfunction: a driving factor in Alzheimer's disease? J. Neurochem. 140, 703–717.
Wiley, J.C., Pettan-Brewer, C., Ladiges, W.C., 2011. Phenylbutyric acid reduces amyloid plaques and rescues cognitive behavior in AD transgenic mice. Aging Cell 10, 418–428.
Yanagida, K., Okochi, M., Tagami, S., Nakayama, T., Kodama, T.S., Nishitomi, K., Jiang, J., Mori, K., Tatsumi, S., Arai, T., Ikeuchi, T., Kasuga, K., Tokuda, T., Kondo, M., Ikeda, M., Deguchi, K., Kazui, H., Tanaka, T., Morihara, T., Hashimoto, R., Kudo, T., Steiner, H., Haass, C., Tsuchiya, K., Akiyama, H., Kuwano, R., Takeda, M., 2009. The 28-amino acid form of an APLP1-derived Abeta-like peptide is a surrogate marker for Abeta42 production in the central nervous system. EMBO Mol. Med. 1, 223–235.
Yip, C.M., McLaurin, J., 2001. Amyloid-beta peptide assembly: a critical step in fibrillogenesis and membrane disruption. Biophys. J. 80, 1359–1371.
Yoshida, H., Okada, T., Haze, K., Yanagi, H., Yura, T., Negishi, M., Mori, K., 2000. ATF6 activated by proteolysis binds in the presence of NF-Y (CBF) directly to the cis-acting element responsible for the mammalian unfolded protein response. Mol. Cell. Biol. 20, 6755–6767.
Zheng, L., Cedazo-Minguez, A., Hallbeck, M., Jerhammar, F., Marcusson, J., Terman, A., 2012. Intracellular distribution of amyloid beta peptide and its relationship to the lysosomal system. Transl. Neurodegener. 1, 19.